Lab on a Chip

Asphaltenes yield curve measurements on a microfluidic platform

Journal:	*Lab on a Chip*
Manuscript ID:	LC-ART-05-2015-000547.R2
Article Type:	Paper
Date Submitted by the Author:	18-Aug-2015
Complete List of Authors:	Sieben, Vincent; Schlumberger, Novel Fluid Analysis Tharanivasan, Asok; Schlumberger, Ratulowski, John; Schlumberger, Mostowfi, Farshid; Schlumberger, DBR - Novel Fluid Analysis

Asphaltenes yield curve measurements on a microfluidic platform

Vincent J. Sieben, Asok Kumar Tharanivasan, John Ratulowski and Farshid Mostowfi*

Schlumberger Canada Limited, DBR Technology Center, 9450 17th Avenue, Edmonton, Alberta, T6N 1M9, Canada

Abstract

We describe a microfluidic apparatus and method for performing asphaltene yield measurements on crude oil samples. Optical spectroscopy measurements are combined with a microfluidic fluid handling platform to create an automated microfluidic apparatus to measure the asphaltene yield. The microfluidic measurements show good agreement with conventional wet chemistry measurements as well as available models. The initial absorbance of the oil is measured, and asphaltenes are removed from the oil by the gradual addition of n-alkane, which leads to flocculation and subsequent filtration. The absorbance of the de-asphalted oil (maltenes) is then measured and the initial asphaltene content is determined by the change in absorbance. The solubility of asphaltenes are evaluated by varying the titrant-to-oil ratio (e.g., n-heptane-oil), which induces no, partial or full precipitation of asphaltenes depending on the chosen ratio. The absorbance of the filtrate is measured and normalized to the maximum content to determine the fractional precipitation at each ratio. Traditionally, a yield curve comprised of 20 such ratios would require weeks to months to generate, while consuming over 6L of solvent and more than 100g of crude oil sample. Using the microfluidic approach described here, the same measurement can be performed in 1 day, with 0.5L of solvent and 10g of crude oil sample. The substantial reduction in time and consumables will enable more frequent asphaltene yield measurements and reduces its environmental impact significantly.

*Corresponding author. Tel: +1 780 577 8341; E-mail: fmostowfi@slb.com

Introduction

Asphaltene precipitation and deposition is a major impediment in production, transportation and processing of reservoir fluids. Unexpected precipitation and the subsequent potential for deposition of asphaltenes can cause reservoir impairment, plugging of wells and flowlines, as well as fouling issues and processing challenges for surface facilities [1]. However, the mechanisms of agglomeration and deposition are not fully proven [1, 2] with only a few available predictive models [3]. Asphaltenes are a sub-component of crude oil that are conventionally defined as being poorly soluble in n-alkanes (ex. n-heptane), and highly soluble in aromatic solvents (ex. toluene) [4]. Asphaltenes precipitate due to a shift in solubility matrix caused by a change in pressure, temperature, or composition of the oil [5-8]. For example, simply combining two incompatible oils may initiate precipitation through a change in composition; even though, both stand-alone samples have asphaltene fractions that otherwise remain stable in solution [9, 10]. Optimal flow assurance requires frequent and accurate fluid characterization and asphaltene phase behavior studies for each crude sample. Quantitative measurements that describe the degree of asphaltene precipitation in response to varying perturbations, aid in understanding the general behavior of these diverse aggregates and help mitigate or prevent costly remedial techniques to remove the problematic material.

Asphaltenes are a complex mixture of different molecules with varying solubility parameters, ranging from least soluble or most unstable and first to precipitate, to most soluble or most stable and last to precipitate sub-fractions. The solubility profile of the asphaltene fraction is represented by the yield curve. A yield curve shows the amount of asphaltenes precipitated as the ratio of the solvent/precipitant mixture is changed. A number of techniques may be used to detect and measure the extent of asphaltene precipitation, including: visual observation [11], absorption and fluorescence spectroscopy [12], light scattering [6], conductivity [13], filtration [14], viscosity [15] and the conventional gravimetric approach [16]. Typically, the maximum asphaltene content of a crude oil is measured at a heptane-crude oil volume ratio of 40. As the amount of n-alkane (or titrant) is reduced, a fraction of the total amount of asphaltene precipitates while the remainder stay in solution due to partial solubility. An asphaltene yield curve is a graph that shows the amount of precipitated asphaltenes as a function of titrant concentration [2]. A yield curve contains valuable information about solubility or phase separation of asphaltenes; notably the precipitation onset point, or the alkane-to-oil ratio at which the asphaltene precipitation begins. Although the yield curve provides meaningful data

for modelling asphaltene behavior [4, 5, 17-19], the cost and time required to complete the analysis are generally prohibitive to be performed routinely using existing methods.

The applications of microfluidics in the oil and gas industry has grown substantially in recent years. Various methods for measuring asphaltene content/properties [20-25], phase behavior [26-28], gas-oil-ratio [29], solvent diffusion [30, 31] and micro-models [32, 33] have been published, uncovering a completely new field of relevance for microfluidic research. Bowden et al. demonstrated one of the first separations of asphaltenes on a microfluidic chip [22, 23]. In their early work, they fractionated hydrocarbons using an H-Cell microfluidic platform so they could rapidly and continuously mix the oil with hexane. The device allowed removal of the high molecular weight species from the apolar components that could then be directly used on a GC [22]. Although Bowden et al. was initially interested in the lighter fractions of the oil (free of asphaltenes), they remarked on the potential utility of microfluidics to evaluate the solubility of asphaltenes analogous to precipitation onset titration. The later work by Bowden et al. coupled UV-Vis spectroscopy with the H-cell microfluidic device to determine the asphaltene content and carboxylic acid content, demonstrating the potential utility of microfluidics for characterization of oil composition [23]. At nearly the same time, Mostowfi et al. were also investigating an approach to determine asphaltene content using UV-Vis absorbance, and comparing the optical data to the traditional ASTM D6560 (IP 143) method for 26 crude oil samples [34]. The data showed a strong linear correlation between optical absorbance and asphaltene content for a large sample set that covered a wide range of geographic locations. Schneider et al. combined the optical technique with a microfluidic platform for rapid asphaltene content measurement on 38 crude oil samples, and demonstrated that a single asphaltene content measurement could be made in less than 30 minutes as opposed to days [20]. Sieben et al. continued the work, expanding to 52 crude oil samples with a larger operating range capable of measuring asphaltene contents up to 15 wt.% [24]. Recent work by Hu and Hartman utilize microfluidics to investigate deposition of asphaltenes in porous media or packed bed reactors (PBR) [21, 25]. By coupling optical analysis (UV-Vis) to a micro-PBR, they were able to study the influence of Reynolds number on asphaltene deposition in a rapid manner. Microfluidics have been successfully applied for the separation of asphaltenes, the measurement of asphaltene content and recently the study of asphaltene aggregation and deposition behavior.

In this work, an optical microfluidic apparatus and method for asphaltene content measurement described earlier [20, 24, 34], is augmented to perform solubility measurements (yield curve). The underlying principles of the optical detection have been addressed in previous work [34], where it was established that asphaltene optical absorbance in the visible range correlated linearly with

conventional asphaltene weight measurements based on ASTM-6560 [35]. Briefly, the initial absorbance of the oil is measured before asphaltenes are precipitated. Next, the addition of excess n-alkane (e.g. n-heptane) induces asphaltene precipitation and the aggregates are filtered out of solution. Subsequently, the absorbance of the de-asphalted oil (i.e., maltenes) is measured and the maximum asphaltene content is determined by the change in absorbance through the established correlation [20, 34]. The ability to rapidly measure asphaltene content using the microfluidic approach may remove the throughput bottlenecks associated with conventional yield curve measurements.

Here we extend the functionality of the microfluidic asphaltene measurement by varying the titrant-oil ratio to evaluate the solubility of asphaltenes. When n-heptane is mixed with oil sample at various ratios, it will induce a partial or fractional precipitation of asphaltenes, depending on the chosen ratio. Mixing of oil with n-heptane is achieved in a microfluidic mixer, which employs a static mixing principle based on fluid lamination and diffusion. After mixing, the fluid is passed through a long microfluidic channel referred to as “reactor”. This channel allows sufficient time for the potential precipitation of adequately sized asphaltenes particles before the fluid stream reaches the filtration unit. While the microfluidic chip contains the core functionality of mixing the fluids, precipitating asphaltenes and filtering the precipitate, peripheral equipment are required in order to drive and condition the fluids and perform the optical analysis. As shown in figure 1, oil sample is loaded manually in the sample loop from where it can be automatically pushed into the microfluidic chip by a toluene-filled syringe. A second syringe dispenses n-heptane into the core microfluidic chip at a particular flow rate matched to the sample-pushing flow rate so that the desired mixing ratio is achieved. Heptane and oil sample are combined on the microfluidic chip in the mixer section, which might cause some or all asphaltenes to precipitate, depending on the mixing ratio. Asphaltene aggregates are held back in the subsequent filtration section while the permeate is guided towards a second mixing chip, based on the same mixing principles as described above. Figure 1B is a photograph of the designed core microfluidic chip used in this study. Figure 1C shows a photograph of the chip while asphaltene particles are precipitating in the channel.

The second mixer unit is an important addition to the previous work described in reference [20], which was originally designed for high dilutions (i.e. addition of excess n-heptane to oil provides sufficient dilution for optical measurement). However, in this work, measurements are made at low dilution ratios to establish the complete yield curve. At a low heptane dilution, the permeate is predominantly a dark fluid, which produces exceedingly high optical absorbance values for the fixed pathlength of the flow cell. Hence, the dark permeate is diluted with adequate amount of toluene so

that the absorbance of deasphalted oil at low dilution ratios is within the spectrometer's detectable range. The output from the second mixer stage (i.e. the diluted permeate) is then passed through the optical flow cell, where the absorbance spectrum of the fluid is measured. Based on the absorbance, and the correlation relating absorbance and asphaltene content, the asphaltene yields for various heptane-oil ratios can be determined. The use of such microfluidic systems to perform resource intensive studies on asphaltene solubility will greatly improve data quality through automation and reduce the labor and time associated with conventional approaches.

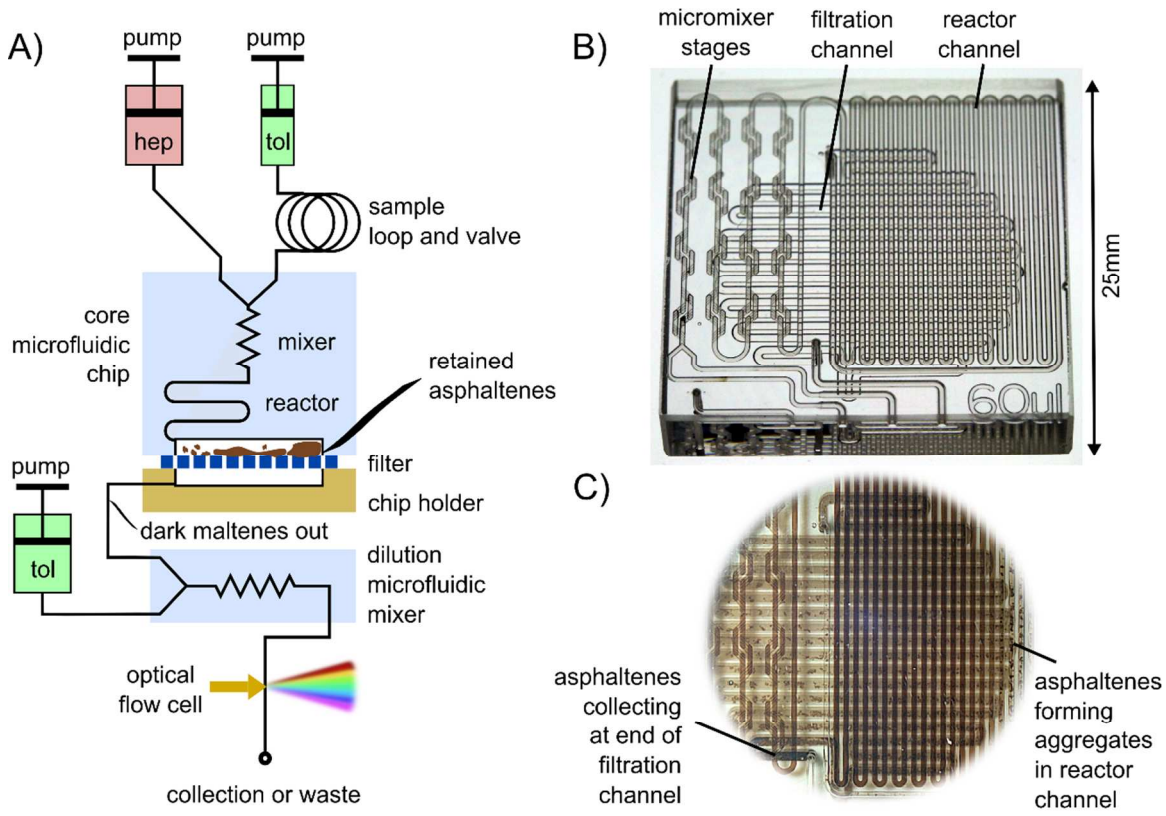

Figure 1: A) Simplified flow diagram to obtain an asphaltene precipitation yield curve using a microfluidic system; the filtration aspects of the chip are shown in cross-sectional view. Crude oil and heptane are mixed at a user selected volumetric ratio and asphaltenes precipitate in the reaction unit. Asphaltene aggregates are screened by the filter membrane on the lower level of the chip. Permeate is then diluted with toluene if required and the optical absorption is measured. B) Core microfluidic chip: photograph of empty glass chip containing mixer, reactor and filter channels. C) Photograph of core chip embedded in the chip holder during operation; top view that shows asphaltenes are retained by the filter membrane (in the paper plane), and usually collect at the end of the filtration channel filling gradually to the inlet.

Methods and Materials

Sample set

Six stock tank oil samples were evaluated in this study, spanning a range of asphaltene contents as listed in table 1. Saturates, aromatics, resins and asphaltenes (SARA) contents for crude oils A, B and C were obtained from reference [36]. The SARA fractions for crude oils D, E and F were measured using a modified ASTM D6560 (IP 143) method and a modified ASTM D4124, described elsewhere [19, 34]. The solvents for the microfluidic asphaltene apparatus were HPLC grade toluene (CAS # 108-88-3) and n-heptane (CAS # 142-82-5), purchased from Fisher Scientific (NJ, USA).

Table 1: Composition and densities of crude oils used in this study (1atm and 20°C).

		composition (wt.-%)				
sample	**°API**	**saturates**	**aromatics**	**resins**	**n-C7 asphaltenes**	**recovery**
crude oil A	29.5	61.6	18.4	13.5	6.1	99.6
crude oil B	16.5	38.4	29.8	25.8	6.8	100.8
crude oil C	31.2	63.1	20.2	13.3	3.7	100.3
crude oil D	29.4	50.3	24.8	22.6	1.1	98.8
crude oil E	21.1	40.2	27.1	23.9	8.5	99.7
crude oil F	28.5	54.4	21.9	18.8	4.3	99.4

Microfluidic chips

Two glass microfluidic chips were used in this study, both manufactured by Dolomite (Royston, UK). The first chip included a y-junction for introducing the oil sample and n-heptane (titrant), several micro-mixer stages to reduce cross-stream diffusion lengths, a serpentine reactor to induce a time delay for reaction kinetics, and an open-face filtration channel that interfaced with porous membrane for filtration and removal of asphaltene aggregates. The filtered mixture was then fed into the second microfluidic chip, which incorporated a 3-way y-junction to further dilute the sample with toluene. The second chip also incorporated several micro-mixer stages for creating a homogeneous deasphalted oil-toluene mixture for downstream optical analysis. Conventional photolithography techniques were used to fabricate the microfluidic chips; i.e. lithography, isotropic etching and temperature annealing. Nominal cross-sectional dimensions of microchannels were (depth by width): 125µm x 350µm (large

channels) and 50µm x 125µm (small channels) for the mixer stages; 250µm x 370µm for the reactor channel; 175µm x 350µm for interconnecting channels; and 200µm x 600µm for the open-faced (i.e. not capped) filtration channel. The first core chip had an internal volume of 51µL plus the reactor section that could be 10, 20 or 60µL depending on design. The second dilution chip had an internal volume of 8µL.

To ensure that oil and heptane are well mixed, the chip incorporates 16 micro-mixers that operate similarly to split and recombine mixers, described in Nguyen and Wu [37]. These mixers cut down on the inter-stream diffusion distances substantially and mixing occurs much more rapidly. In this particular mixer, the diffusion length is reduced 8 times after each mixer stage. For a typical flowrate of 80µL/min, the manufacturer recommends 6 micro-mixer stages, which is much less than the number of stages incorporated in our device, thereby ensuring a well-mixed stream entering the reactor. We have confirmed a homogenous mixture with microscopy at a ratio of 40:1 (n-heptane-oil) after 4-8 mixer stages, far before entering the reactor.

The reactor length or volume is an important parameter to be considered as together with the flow rate it determines the residence time, i.e. the time the asphaltenes are allowed to precipitate after mixing with heptane and before the separation by filtration. In our previous work [20], we showed that Taylor-Aris dispersion of oil sample plugs is a valid description of broadening as the plug traverses our microfluidic channels – indicating that the oil constituents are crossing the axial flow lines enough times to make the model valid. In other words, the cross-sectional diffusion time is sufficiently small compared to the axial transit time as the sample flows through the chip. Schneider et al. determined that asphaltenes diluted in excess toluene have a diffusion coefficient in the range of 5×10^{-6} cm^2/s [12]. The calculated characteristic diffusion time across the reactor channel is approximately 0.8 seconds. Therefore, there is sufficient time for the diffusion of asphaltenes to form aggregates as the axial transit time is usually greater than 5 seconds.

Complete system

A custom made aluminum and polyether ether ketone (PEEK) block or chip holder was used to house the core microfluidic chip. The PEEK section of the chip holder had a micro-machined serpentine channel that was open-faced for permeate collection; it was a mirror image of the core chip filtration channel. The porous filter membrane was compressed between the core microfluidic chip and the PEEK portion of the chip holder as shown in figure 1A. The filter used in this work was a 0.2µm hydrophobic

poly-tetrafluoroethene (PTFE) membrane with an average pore size of 0.2µm for separating the precipitated asphaltenes from maltenes. ASTM standard D6560 recommends the use of WhatmanTM grade 42 filters, which would retain particles larger than 2.5µm [35]. If microscopy methods are used, the precipitation onset is detected when the particle size is about 1µm [9]. Hence, the nominal pore size of the filter (0.2µm) used in this work is more stringent than traditional methods for detecting precipitation. The chip holder also created fluidic connections to external tubing for reagent delivery and collection. The total volume of the assembly was approximately 152µL. For temperature control, the entire setup was placed inside a customized block heating system (QBD4, Grant, UK).

The output from the core chip holder assembly was routed to the second microfluidic chip for post-dilution with toluene. The toluene post-dilution provided a detectable absorbance on the fluids with no or low n-heptane dilution for spectrometric measurements, ensuring that the measured deasphalted oil absorbance was in the linear range with a value less than two [38]. The optical absorbance of the toluene diluted permeate was measured with a 2.5mm path length flow cell (SMA-Z-2.5-uvol, 2µL internal volume, FIALABs, USA), using a tungsten halogen white-light source (LS-1, Ocean Optics, usable range 360-2500nm) and a UV-VIS spectrometer (HR2000+CG-UV-NIR, Ocean Optics, usable range 200-1100nm).

Three stepper-motor syringe pumps (Mitos Duo XS, part #3200057, Dolomite, UK) were used to pump the toluene, n-heptane and the oil sample plug. Glass syringe sizes were selected based on the desired mixing ratios to maintain smooth flow and minimize the number of syringe refills. Pressure sensors (40PC150G2A, Honeywell, USA) were used to ensure safe operation and also to verify that the automated protocol performed as anticipated. Sample plug loading and injection was accomplished with a rotary valve (Cheminert C22-3186EH, VICI-Valco, USA). Additional valves were used for fluid routing. The maximum operating pressure of the system was theoretically 10bar, limited by the glass syringe, the valves and the filter membrane holder. The system was operated within 6bar for reliability and safety reasons. The sample and solvents were filtered using 10µm and 2µm in-line frit cartridges, respectively. When required, samples were pre-filtered with a 0.2µm PTFE syringe filter to remove excess fines and particles. All fluidic components were connected using fluorinated ethylene propylene (FEP) tubing that had an inner diameter of 250µm. The whole system operation was controlled and automated with custom electronics and a personal computer running LabVIEW 8.6 (National Instruments, USA) software. The program also captured and analyzed the absorbance spectrum over time for data processing and presentation.

Procedure

For each chosen n-heptane to oil volume ratio, a "run" is performed where n-heptane and oil are mixed, insoluble asphaltenes are precipitated and filtered, and the permeate is optionally diluted with toluene and passed through the spectroscopy flow cell, see figures 1 and 2. The post-dilution amount is determined by targeting for a final solvent dilution of about 40:1 (solvent:oil) based on the three pump flow rates. Flow conditions are maintained until a stable absorbance spectrum can be acquired. Each run produces data corresponding to a single point on the asphaltene solubility curve (yield curve) and the entire curve is mapped out by multiple runs with various heptane to oil volume ratios. Hereafter, we define the heptane to oil volume ratio as the heptane-oil ratio (R).

Each yield curve contains an experimental run with a heptane-oil ratio near zero (neat oil, where most asphaltenes are soluble) and a run with maximum precipitation, often at a heptane-oil ratio of approximately 40. Based on these two key runs (no precipitation and maximum precipitation) the other data points are scaled and plotted as fractional asphaltene precipitation versus heptane-oil ratio, as in equation 1:

$$x(R) = \frac{A_{asph\,@\,R}}{A_{asph\,@\,R_{\max}}} = \frac{A_{malt\,@\,R=0} - A_{malt\,@\,R}}{A_{malt\,@\,R=0} - A_{malt\,@\,R_{\max}}} \quad (1)$$

where x(R) is the fractional asphaltene precipitation at the heptane-oil ratio R, $A_{asph@R}$ is the asphaltene absorbance at R, $A_{asph@Rmax}$ is the maximum asphaltene absorbance (usually around R=40), $A_{malt@R=0}$ is the filtrate absorbance with toluene only dilution (i.e. neat oil absorbance), $A_{malt@Rmax}$ is the minimum filtrate absorbance at Rmax (i.e. maximum asphaltene precipitation) and $A_{malt@R}$ is the filtrate absorbance at the heptane-oil ratio R. Each absorbance value in equation 1 is the difference between the absorbance value at wavelengths of 600nm and 800nm, as established in previous work [34].

The characteristic absorbance for each heptane-oil ratio is adjusted to an equivalent solvent dilution of 40:1, based on the volumetric flow rates of the three syringes during a particular run. For example, at R=5, the pump flow rates may be 75µL/min n-heptane, 15µL/min oil sample and 600µL/min post-dilution with toluene. If the characteristic absorbance of the filtrate was recorded as 0.300au (600nm – 800nm), then the value used in equation 1 would be 0.337au based on the 1.122 dilution adjustment to an R=40 equivalent. The dilution normalization is calculated based on the ratio of flow

rates for R=5 to R=40; dilution norm. = (75µL/min+15µL/min+600µL/min) / (15µL/min+600µL/min) = 1.122. If desired, fractional precipitation values x(R) at each ratio can be converted to weight percentages using the maximum asphaltene absorbance and the correlation in reference [20]. The process of creating a yield curve is graphically summarized in figure 2.

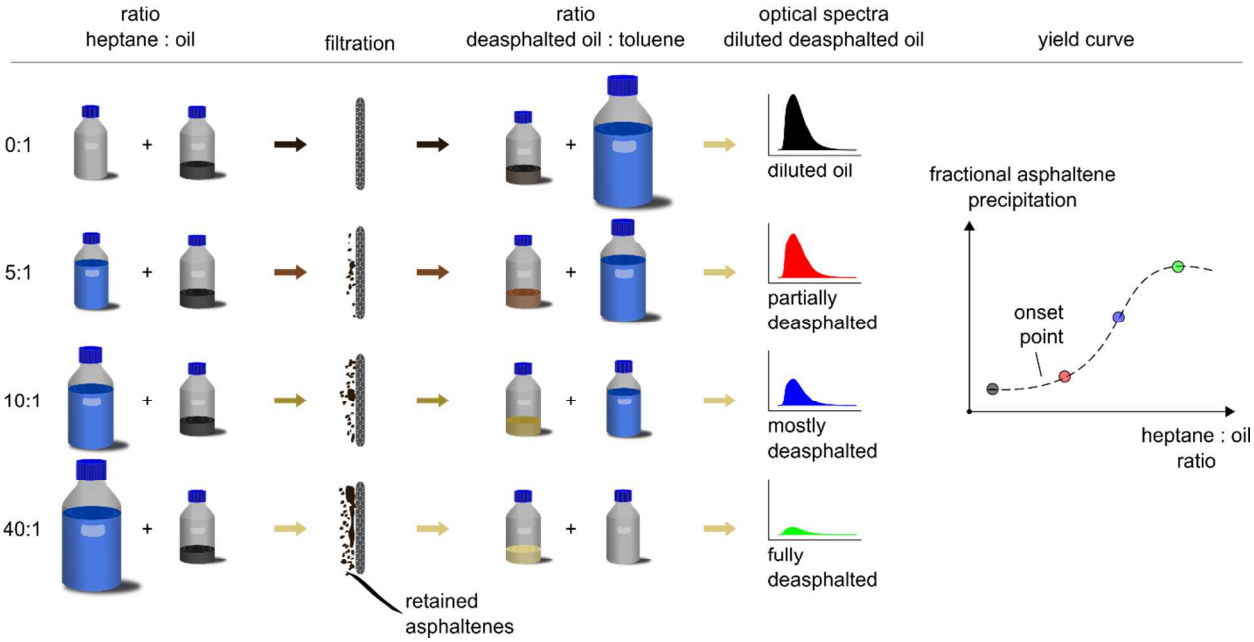

Figure 2. Schematic of experimental procedure for acquiring the asphaltenes yield curve on the microfluidic device.

Results and Discussion

Obtaining the yield curve from raw data

The yield curve for an individual crude oil sample is generated by sweeping through a range of heptane-oil ratios and measuring the optical absorbance of the filtrate. Ten to twenty individual experimental runs are performed per yield curve. A subset of the data generated by the microfluidic system for crude oil-A is shown in figure 3. The data shows the optical absorbance and pressure profiles plotted versus time for 6 different ratios. At a heptane-oil ratio of 0.25 (labelled "< asphaltenes onset"), the pressure profile shows a gradual increase and decrease as the oil plug passes through the filter membrane. The step drop and rise in pressure that occurs every 550 seconds are the automated syringe refills, also synchronized with the absorbance transients. The absence of stochastic pressure spikes throughout the filtration process indicates that solvent-induced asphaltene aggregation has not yet occurred. The heptane-oil filtrate is then diluted with toluene and an optical absorbance measurement is performed. The average absorbance of the diluted filtrate at the plateau is 0.736au.

In order to determine if the asphaltenes precipitated at the dilution ratio of 0.25, the absorbance of the toluene diluted filtrate is compared with the absorbance of the neat oil diluted with toluene (R=0). The measured absorbance of toluene diluted neat oil was 0.800au. Although the difference in absorbance (0.064au) indicate that asphaltenes precipitate at the dilution ratio of 0.25, this may be an artifact due to the presence of pre-existing asphaltene aggregates in the neat oil. It is worthwhile to note that the absorbance for neat oil is measured by pre-diluting the oil sample with toluene. In the pre-dilution experiment, the oil was mixed with toluene before filtration by injecting toluene instead of heptane at the chip inlet. The addition of toluene before filtration increased the solubility of the mixture and dissolved any suspended asphaltene aggregates. The mixture was then passed through the filter membrane and an absorbance of 0.800au was measured (R=0). A post-dilution experiment was conducted as well using the lowest heptane-oil ratio run (R=0.01). In this case, the volumetric flow rates of oil and n-heptane were 50µL/min oil and 0.5µL/min, respectively. The heptane-oil mixture was filtered and then post-diluted with toluene to perform an absorbance measurement. The filtrate had an absorbance of 0.760au. At such a low heptane volume concentration of 1%, the addition of n-heptane is unlikely to induce asphaltene precipitation. Post-dilution with toluene was also performed at the heptane-oil ratio of 0.05. A similar absorbance of 0.760au was observed. Hence, the difference between the pre-dilution and post-dilution absorbance values at low dilution ratios suggest the presence of pre-existing asphaltene aggregates in the neat oil. Crude oil-A was the only sample in

this dataset that showed a difference between pre-dilution with toluene (R=0.0) and post-dilution with toluene (R<0.05). As a result, we modified the microfluidic method to use the pre-diluted run/case as the zero precipitation absorbance value to account for the presence of suspended aggregates.

Figure 3 shows that solvent-induced asphaltene onset was detected between the heptane-oil ratios of 0.6 and 1.0 for crude oil-A, labelled "@ asphaltenes onset". The aggregation of asphaltenes is first detectable at R=0.6, noted by the combined effects of a drop in steady-state absorbance and the fluctuating pressure pattern. The absorbance of the filtrate decreased from 0.739au (R=0.25) to 0.709au (R=0.6). Also, the absorbance standard deviation on the plateau was 0.039au at R=0.6, which is the largest of all heptane-oil ratios. Typically, we observe a standard deviation of less than 0.015au for the plateau measurement. This may indicate that asphaltene aggregate size is slightly below the 0.2µm filter pore size. A fraction of the particles are small enough to pass through the filter, but large enough to result in light scattering as they pass through the optical flow cell [6]. Additionally, at onset we often noted a rising pressure profile with momentary spikes in pressure as the heptane-oil filtrate passed through the membrane. The fluctuating pressure patterns arose from asphaltene aggregates clogging the filtration microchannel as the membrane filtered and collected asphaltenes on the topside open face channel. At low ratios, the clogs occurred at the start of the of the filtration channel just after the reactor. Pressure build-ups from the continuously flowing viscous heptane-oil mixture would dislodge and clear these channel blockages, sweeping the aggregates to the end of the filtration channel. The repeating pattern of block-pressurize-dislodge-block produced large pressure transients at low ratios. When the heptane-oil ratio was increased above the asphaltene onset (R=1.0 to R=1.75), the pressure rise started earlier, was more systematic and was higher in magnitude. More asphaltenes were precipitated and filtered, leading to a greater degree of membrane fouling and a rise in pressure. The increase in system pressure, which was due to mixer clogging as well as membrane fouling, was tolerated up to 6 bars, beyond which the system was automatically stopped. The precipitated asphaltenes in the microchannels and the membrane were then dissolved using toluene. The removal of asphaltenes from the crude oil also produced a lower filtrate absorbance of 0.588au, 0.537au and 0.430au for heptane-oil ratios of 1.0, 1.2 and 1.75, respectively.

At higher heptane-oil ratios (R>2), the precipitant driving force is sufficient for rapid aggregation. When heptane was added in excess to the oil, R=40 (labelled ">> asphaltenes onset") – figure 3, an early pressure rise was observed with a low characteristic absorbance of 0.264au. The smooth and rapid pressure rise was attributed to a systematic dead-end filling of the filtration channel with asphaltenes as the heptane-oil mixture was filtered.

After gathering data for the desired number of heptane-oil ratios, the optical absorbance spectra were processed to produce the fractional yield data as shown in figure 4A as per equation 1. Specifically, the asphaltenes absorbance for each heptane-oil ratio was calculated by subtracting the filtrate absorbance at that heptane-oil ratio from the absorbance of the neat oil (pre-diluted with toluene, R=0). The asphaltene absorbance value for each heptane-oil ratio were then normalized to the asphaltene absorbance at the maximum precipitation to obtain fractional precipitation yield.

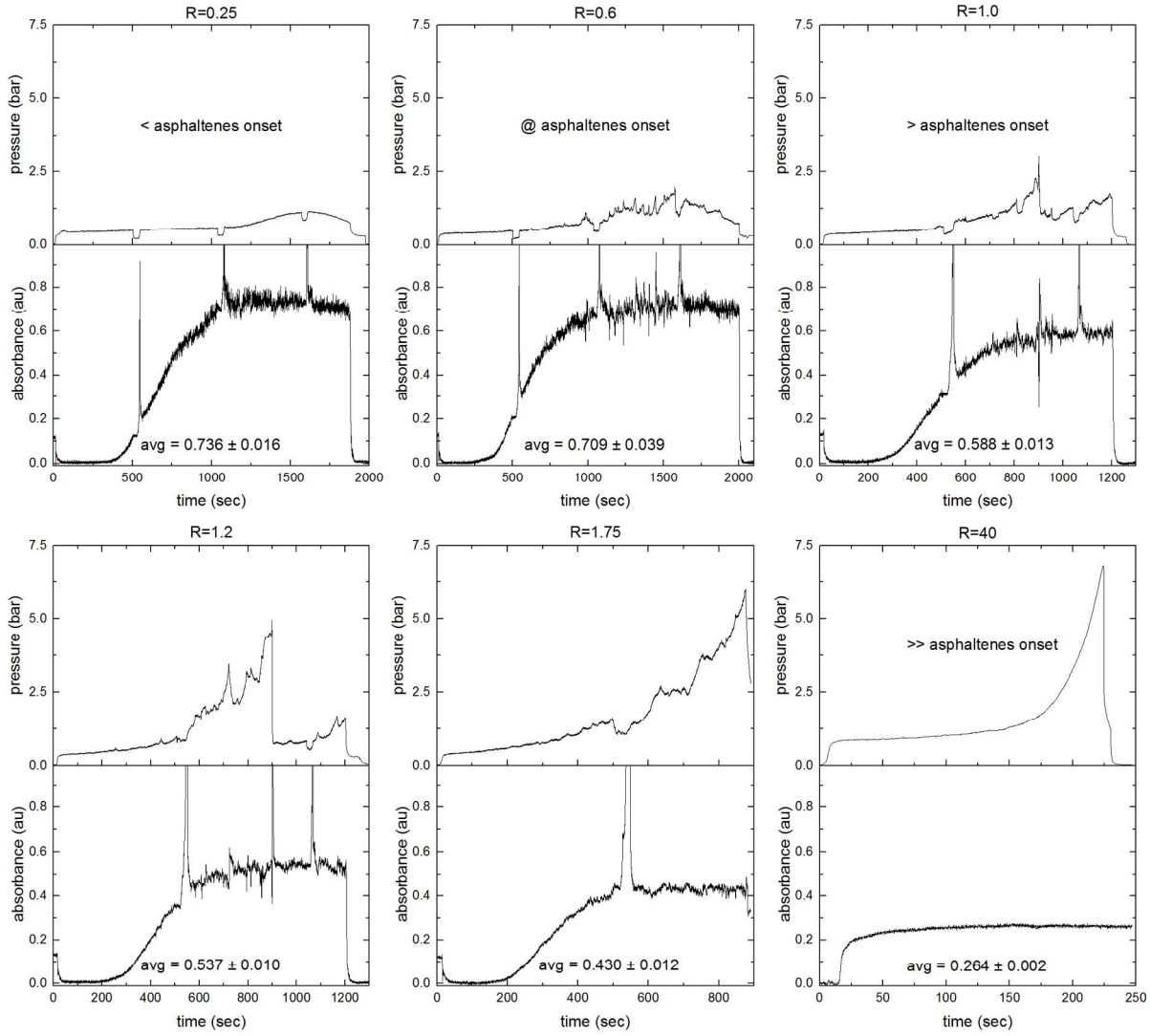

Figure 3. Raw data produced by the microfluidic apparatus for crude oil-A. Chip inlet pressure and optical absorbance (600nm minus 800nm) versus time for various heptane-oil ratios.

Comparison of conventional and microfluidic methods

The microfluidic yield data is compared to conventional yield data for Oil-A and Oil-B, shown in figures 4A and 4B, respectively. Conventionally measured yield data for crude oils A and B were published in reference [36]. Oil-A microfluidic data showed a reasonable agreement with the conventional data, compared in figure 4A. The asphaltene onsets were similar, with the microfluidic onset at a heptane-oil ratio of 0.6 and the conventional onset at 0.5. As the heptane percentage was increased in the mixture, both microfluidic and conventional yield data showed similar front-ends; a steep rise, then a levelling-off point at a heptane-oil ratio of 3, followed by a shallow rise to the maximum precipitation. However, for heptane-oil ratios greater than 30 there was a slight deviation; the microfluidic data tended downward while the conventional data showed a plateau. We discuss the microfluidic downward trend under the section of infinite dilution below. The data for crude oil-B in figure 4B showed asphaltene onsets were nearly identical at a ratio between 2.0 to 2.5. In this example, the conventional data had a more gradual rise to the maximum precipitation compared to the microfluidic measurements. A large degree of scatter after a heptane-oil ratio of 20 for the conventional measurements makes it difficult to precisely determine the maximum precipitation yield. For both crude oils A and B, the conventional gravimetric data and the microfluidic optical data are similar in precipitation onset and curve shape.

The slightly higher microfluidic onset compared to the conventional onset for oil-A, 0.6 versus 0.5, may result from the microfluidic method over-estimating the solubility of asphaltenes at low ratios ($R<2$). Maqbool et al. demonstrated that near asphaltene precipitation onset ($R\approx0.5$-2), the aggregation process may take from minutes to thousands of hours depending on the crude oil [39]. In their work, detection of precipitation onset was based on the observation of particles greater than 0.5µm using light microscopy. Maqbool et al. studied two oils and showed that the precipitation onset was only detectable after 1000-5000 hours for a heptane volume of ~40% ($R=0.67$). However, with a slightly higher heptane volume of ~55% ($R=1.22$), one of the oils had noticeable precipitation in less than a minute. The other oil required a heptane volume of ~60% ($R=1.50$) to induce precipitation within minutes. The study highlights the importance of aggregation kinetics in detecting asphaltene precipitation onset – there is an exponential dependence on particle formation rate and precipitant concentration. In our study, the slower flow rates used at low heptane-oil ratios provide increased residence time in the reactor channel of the chip. The time for asphaltene aggregation on chip ranges

from 30 seconds (R=0.4) to 0.5 seconds (R=80). Therefore, the microfluidic method is likely over-estimating the solubility of asphaltenes near onset by not providing enough time for aggregates to grow. Asphaltene precipitation onset may physically occur at slightly lower heptane-oil ratios than our measured onsets. Longer time delays in the reactor channel or smaller filter pore-sizes (~10-50nm) could be used to improve the detection of precipitation onset. Even when considering kinetics effects, the 0.1 difference between onsets is within experimental error.

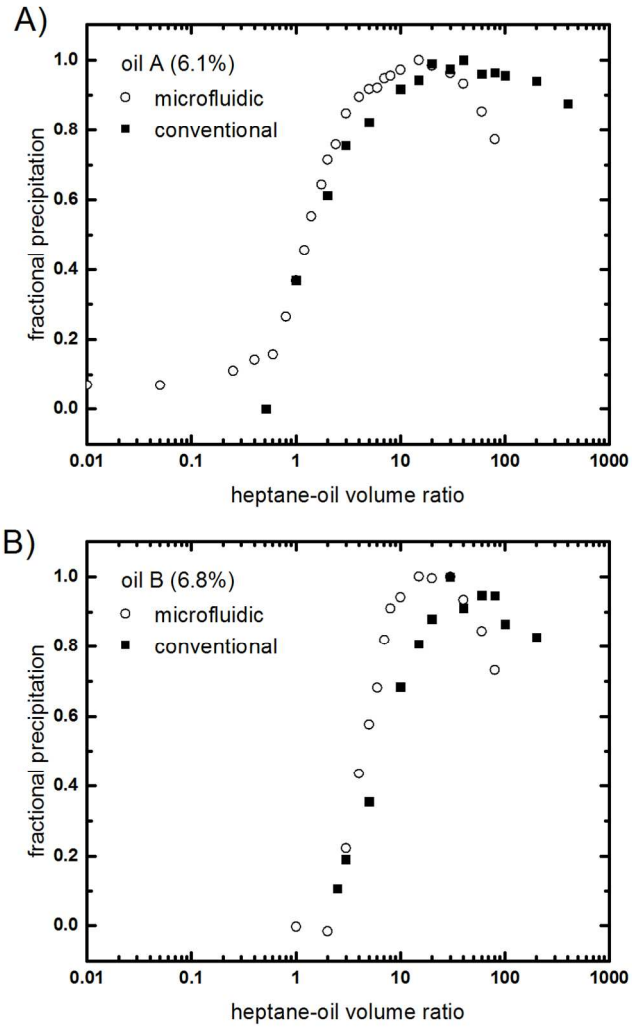

Figure 4. Comparison of asphaltene yields measured from conventional and microfluidic methods. The traditionally measured maximum asphaltene content of the oil samples (in wt.-%) is provided in brackets.

Sample set yield data

The precipitation yield data for crude oils A, B and C are shown in figure 5A. Fractional precipitation is plotted versus heptane-oil volume ratio. The samples in figure 5A are shown together to highlight that the onset point, general shape and maximum precipitation are easily discernible and different for each oil sample as measured by the microfluidic method. To evaluate the lower and upper operational limits of the microfluidic method, yield data for crude oils D and E are also shown in figures 5B and 5C. For the waxy crude, oil-F, measurements are performed at 65°C and the yield data is shown in figure 5D.

The yield curve in figure 5B was acquired from the relatively low asphaltene content oil – crude oil-D with an asphaltenes content of 1.1wt.-%. A total of 19 microfluidic experiments were conducted at room temperature, 22-24°C, with varied heptane-oil ratios ranging from 0 to 80. As expected, at low heptane concentration (R<0.6), the fractional precipitation was virtually zero. At a heptane-oil ratio of 0.6, the first portion of asphaltenes aggregates form and were separated by the porous membrane; therefore, we consider the heptane-oil ratio of 0.6 as the onset point (similar to the method above). As the percentage of heptane increased after the onset point, so did the amount of precipitated asphaltenes. The asphaltene yield reached a maximum value at a heptane-oil ratio of 40, beyond which the precipitated amount decreased slightly. This decrease can be associated with an increase in solubility of the asphaltenes in heptane at infinite dilutions, where aggregate formation is hindered by relatively large asphaltene inter-molecular distances [4, 40]. Heptane-oil ratios greater than the maximum were selected to ensure the maximum precipitation was measured and to investigate the decline after the peak. The optical setup used here was limited to a heptane-oil ratio of approximately 100, where the diluted oil absorbance signal was typically outside the viable measurement range and approached the system noise limits. Longer optical path lengths may be used to measure the precipitation yield for heptane-oil ratios beyond 100.

Two technical problems were encountered when acquiring the yield curve for crude oil-D. First, when unfiltered oil was analyzed with the microfluidic system, transmembrane pressure exceeded 6bar; thereby, making steady state optical readings difficult to obtain. This only occurred for very low mixing ratios. However, when the oil sample was pre-filtered with a 0.2µm PTFE syringe filter, the maximum observed pressure was reduced sufficiently to permit data collection at low heptane-oil ratios (R<5). This suggests that the crude oil-D sample had notable fines and/or precipitated wax that led to early

membrane clogging. Samples that produce significant transmembrane pressures, greater than 5 to 6 bar, should be pre-filtered to remove the particulate matter. If the pressure build-up resulted from wax, temperatures above the wax appearance temperature can be used for measuring the yield curve. In either case, pre-filtration using the same pore size and removal of particulate matter, such as wax or fines, did not impact the measured optical absorbance. Second, the system dead-volume (152µL) became appreciable at low mixing ratios. For example, at a heptane-oil ratio of 1, a total volume of 400µL (200µL heptane + 200µL oil) was delivered to the system and Taylor dispersion led to more pronounced sample smearing [41]. This reduced the duration of the optical measurement plateau and in some cases the absorbance signal did not reach steady-state. To achieve a suitable measurement window, it was necessary to increase the injected sample volume from 200µL to 500µL. This solution had two detrimental effects: a) it increased the amount of oil sample and more asphaltenes were deposited on the filter membrane, and b) it made the experimental run times at least 2.5 times longer. At slow flow rates near onset ($R<2$) this was amplified as it took longer to displace chip dead-volume and reach a steady-state; experimental times were approximately 2000 seconds ($R\approx0$) instead of 200 seconds ($R>10$). Although this solved the dead-volume problem for crude oils A-D, samples with higher asphaltene content will not benefit from this solution as the filtration channel may completely fill before the system reaches steady-state.

Figure 5C depicts the yield curve (15 experiments) for the highest asphaltene content sample, crude oil-E, at 8.5wt.-%. The maximum precipitation was at a heptane-oil ratio of 20. Crude oil-E showed a more pronounced leveling off unlike crude oils A - D, as the fractional precipitation differed by less than 0.5% at heptane-oil ratios of 10, 20 and 40. The precipitation onset could not be readily measured for this sample because the apparatus over-pressured before reaching a stable measurement plateau. Even with a larger filter pore size of 1.2µm, rapid clogging occurred for heptane-oil ratios lower than 5 and prevented a steady-state measurement below a heptane-oil ratio of 1. A redesigned chip with a large filtration capacity channel would address this limitation for high asphaltene content crude oils. Fundamentally, we do not anticipate any issues for low or high asphaltene content oils between the microfluidic and conventional approaches.

The final crude oil sample, oil-F with an asphaltenes content of 4.3wt.-% and an appreciable wax content was analyzed. A wax appearance temperature of 32.2°C was measured using cross polarization microscopy [42]. Figure 5D shows the yield curve for this sample measured at 65°C for heptane-oil ratios ranging from 0 to 100. In the case of crude oil-F, the precipitation temperature was chosen at 65°C versus 22-24°C to avoid filter membrane fouling due to wax deposition. The test at elevated

temperature will slightly increase the asphaltene solubility, thereby decreasing precipitation yield and shifting the yield curve. The ability to run solubility analysis at multiple temperatures, for modelling or to evaluate waxy crudes, demonstrates the flexibility of the microfluidic method. The yield curve for this sample exhibited no asphaltene precipitation at low heptane-oil ratios (R<0.3). The precipitation onset occurred at a heptane-oil ratio of 0.4 and the maximum precipitation was at a heptane-oil ratio of 10.

A total of 21 experiments were performed to acquire the yield curve in figure 5D, which required 15 hours of experimental time (10% setup, 90% runtime), 0.435L of solvent and 9.3mL or 8.2g of crude oil sample. The operator was only required for a few hours to setup the device. Using conventional methods, approximately 0.3-0.5L of solvent and 5g of crude oil are required for each point on the yield curve. An entire yield curve would consume over 6L of solvent (a conservative estimate) and more than 100g of crude oil sample based on 20-points. Further, even if multiple runs/ratios were completed in parallel, it would take a trained operator over 5 working days, including drying, to collect all the data in the yield curve [35]. The microfluidic approach results in over an order of magnitude improvement in solvent use with no loss in data quality, thereby reducing the environmental footprint of such measurements.

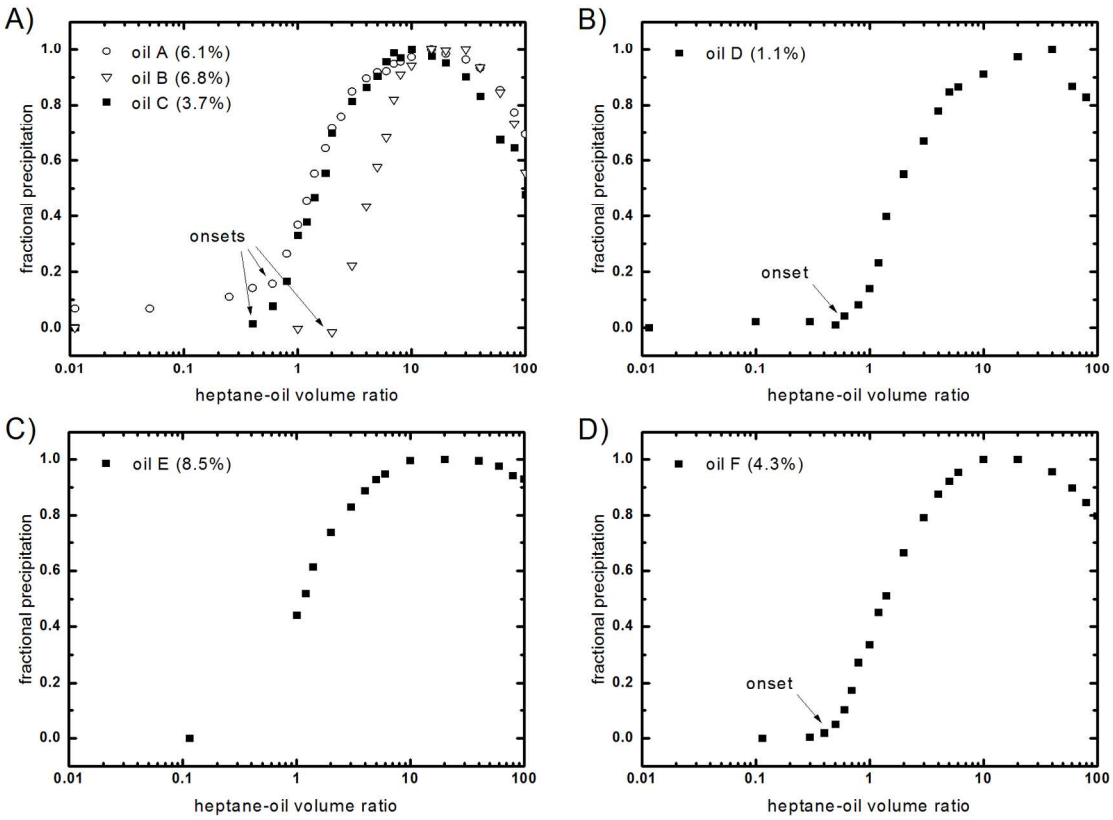

Figure 5. Microfluidic system measured asphaltene yield curves for the six crude oils used in this study. The maximum asphaltene content for each oil is provided in brackets. All data acquired at 22-24°C and 1atm, with the exception of crude oil-F performed at 65°C and 1atm.

Infinite dilution effect

Generally, the microfluidic yield curve data showed a consistent downward trend at high heptane-oil ratios, observed in varying degrees for the six oil samples used in this study. Two main factors contribute to the differences in asphaltene yield at high dilution ratios obtained between the conventional and microfluidic methods.

First, both methods suffer from diminished signal-to-noise ratios (SNRs) at high heptane dilutions. For gravimetrically measured yield data, either vast volumes of solvent or small sample masses must be used to achieve such high dilution ratios. Hence, conventional approaches introduce error via manual dilution and washing steps or by mass measurement limits. For optically measured yield curves, the high dilution ratios produce a fluid with substantially lower absorption of light. The optical path length of a system is usually fixed and designed for a specific dynamic range. The range is constrained by the Beer-Lambert law assumptions and by detector sensitivity; often targeted for measuring an absorption of less than 2au and above the inherent detection noise [38]. In the described system, the standard deviation on a blank measurement was typically +/- 0.005au and the standard deviation on a sample measurement was often +/- 0.015au. The limit-of-detection (LOD) can be defined as 3 times the standard deviation of a blank measurement, which leads to an LOD of +/- 0.015au. For crude oil-F (figure 5D), a heptane-oil ratio of 60 produced a filtrate absorbance of 0.212au. Applying the standard deviation of 0.015au leads to an absorbance range of 0.197-0.227au. The fractional precipitation at R=60 was 89.7% (0.212au) and based on the standard error in absorbance will range from 86.1% (0.227au – less apparent asphaltene filtration) to 93.4% (0.197au – more apparent asphaltene filtration), or +/-3.7% in the fractional precipitation. At higher dilution ratios (R>100), this error becomes more pronounced as the optical absorbance values approach and become comparable to the LOD.

Second, at high dilution ratios, diffusion limited aggregation (DLA) becomes dominant and the significance of asphaltene aggregation kinetics is reduced, or reaction-limited aggregation (RLA) is less dominant. This is important at high heptane-oil ratios because the residence time for the precipitated asphaltenes in the microfluidic reactor is relatively short. For example, the residence time is about 0.5 seconds for a heptane-oil ratio of 80, while the residence time is about 13 seconds at a heptane-oil ratio of 5. Therefore, the aggregates may not have enough time to grow in size beyond the nominal 200nm

filter pore size. Conversely, conventional yield experiments are left for several hours and can be incubated for days or even months, providing sufficient time for aggregation to take place and form adequately sized aggregates [36, 39, 43-45]. Although microchannel mixing processes are much more rapid than conventional bulk mixing approaches [37], DLA may become problematic at exceedingly high dilution ratios. One potential work around would be the implementation of a stop-flow type system with a hold chamber that would allow for user specified long incubation times [41].

Although there are differences between conventional and microfluidic yield data at high dilution ratios, a downward trend may be expected where asphaltenes remain largely dissociated due to infinite dilution. A modified regular solution model described in Appendix A and references [5, 18, 46] was used to compare the modelled yield curve against the microfluidic yield data, shown in figure 6. The experimental microfluidic data closely captures the shape of the model yield curve, including the downward trend at high dilution ratios. The model inputs are the normalised mass fractions of the SARA composition fractions in the crude oil and the average molar mass of self-associated asphaltenes. To cover a wider range of asphaltene molar mass distribution, SARA fractions based on n-pentane precipitated asphaltenes are used in the model (C5-asphaltenes) and the average molar mass of asphaltenes is adjusted to fit the measured precipitation onset. The n-pentane separated asphaltenes were measured on the microfluidic device as having an optical absorbance of 1.12 times the n-heptane separated asphaltenes for crude oil F at a heptane-oil ratio of 40. As the model required the C5-asphaltenes, we applied the C5/C7 microfluidic absorbance ratio to the conventionally measured C7-asphaltenes (4.3wt.-%) and removed the differential amount from the resins fraction (0.5 wt.-%). For crude oil-F, the resulting mass fractions of saturates, aromatics, resins and C5-asphaltenes used in the model are 54.4, 21.9, 18.3 and 4.8wt.-%, respectively. The fitted molar mass of asphaltenes nanoaggregates in crude oil-F was found to be 3185g/mol, which compared reasonably well with the average nanoaggregate mass determined for oils from the same geographic location [19].

We use the term asphaltene nanoaggregates above to describe self-associated stacks of asphaltene molecules as per the Yen-Mullins model [47]. It must be highlighted that 3185g/mol is only a fitting parameter for the modified regular solution model and is best linked to an average nanoaggregate weight and not an average asphaltene molar mass. Wu et al. showed asphaltene molecular weights range from 580-700g/mol and they also determined that petroleum asphaltenes form nanoaggregates that typically contain 6-8 molecules [47, 48]. Based on the above model fitting parameter and molar mass range, Oil-F would contain approximately 4-5 asphaltenes molecules in a nanoaggregate. Overall, the asphaltene yields obtained from microfluidic system matched the

conventionally measured yield data and also follow the model yield trend at high dilutions. We have shown a novel microfluidic approach for determining asphaltenes onset point, as well as, fractional precipitation or yield data. The data generated from our device is useful for probing asphaltene solubility in crude oils and for tuning such models, without the long turn-around times of conventional methods.

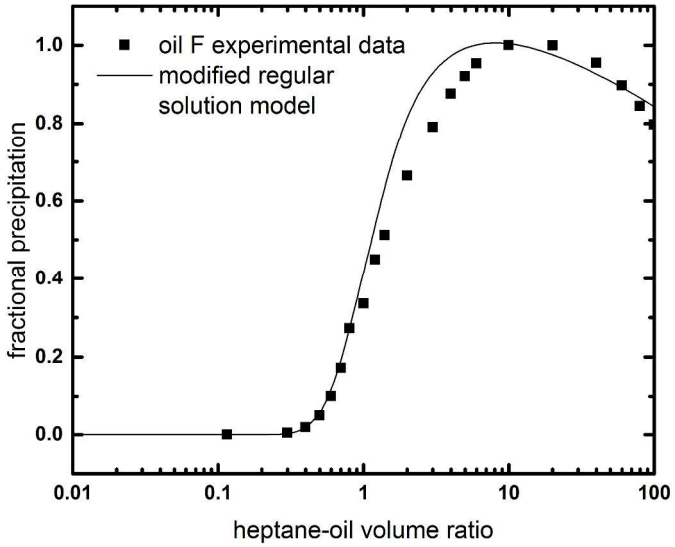

Figure 6. Asphaltene precipitation yields for crude oil-F at 65°C and 1atm, showing the modified regular solution model and microfluidic experimental data.

Conclusions

In this study, we have introduced a microfluidic apparatus for rapidly obtaining the yield curve for a sample of crude oil. The system is built upon a technique for measuring asphaltenes using optical spectroscopy combined with a microfluidic fluid handling platform. To build each yield curve, tens of asphaltene solubility measurements in heptane are completed in one day instead of the several weeks to months required by conventional approaches. The microfluidic system also produced 10-fold less waste, oil and solvent, making the system portable and more cost-effective for such resource intensive studies. We have shown that the precipitation onset and maximum precipitation can be determined from the data and that regular solution models can be tuned to model the data reasonably well. Generally, such microfluidic systems will enable fast, accurate, repeatable and cost-effective solubility measurements for tuning petroleum processes and models.

Acknowledgements

We would like to acknowledge Professor Harvey Yarranton, Dr. Kamran Akbarzadeh, Dr. Simon Andersen and Dr. Shawn Taylor for providing guidance and assistance with asphaltene solubility. In addition, we note our many insightful remarks and discussions on asphaltenes with Laura Magro, Dr. Marc Schneider and Dr. Oliver Mullins. Also, we acknowledge Dr. Jeff Creek and Dr. Jianxin Wang from Chevron for providing crude samples.

Appendix A. Modified Regular Solution Model

The details of the model has been presented elsewhere [5, 46]. Briefly, the modified regular solution model includes a Flory-Huggins entropic contribution from the difference in molecular sizes as well as an enthalpy contribution from regular solution or Scatchard-Hildebrand solubility theory. A liquid-liquid equilibrium is assumed and the equilibrium ratio, K_i^{hl}, for any given component is given by:

$$K_i^{hl} = \frac{x_i^h}{x_i^l} = \exp\left\{ \begin{array}{l} \frac{v_i^h}{v_m^h} - \frac{v_i^l}{v_m^l} + \ln\left(\frac{v_i^l}{v_m^l}\right) - \ln\left(\frac{v_i^h}{v_m^h}\right) + \\ \frac{v_i^l}{RT}(\delta_i^l - \delta_m^l)^2 - \frac{v_i^h}{RT}(\delta_i^h - \delta_m^h)^2 \end{array} \right\} \quad \text{(A1)}$$

where x_i^h and x_i^l are the heavy and light liquid phase mole fractions, R is the universal gas constant, T is absolute temperature, v_i and δ_i are the molar volume and solubility parameter of component i in either the light liquid phase (l) or the heavy liquid phase (h), and v_m and δ_m are the molar volume and solubility parameter of either the light liquid phase or the heavy liquid phase. The terms containing only molar volumes are the entropic contribution and the terms containing solubility parameters are the enthalpic contribution.

Once the equilibrium ratios are known, the phase equilibrium calculations are performed using standard techniques to determine the composition and amounts of heavy and light liquid phases. The amount of heavy liquid phase is considered as the amount of asphaltenes precipitated. To use this model, the mole fraction, molar volume, and solubility parameter of each component in the mixture must be specified. The molar volume is obtained from molar mass and density. In this study, the heptane-oil mixture is characterized into five components: n-heptane, saturates, aromatics, resins and asphaltenes. Pure component properties are used for n-heptane and average properties are used for SARA fractions. The

generalized molar mass and property (density and solubility parameter) correlations for the SARA fractions can be found elsewhere [19].

The modified model also treats the asphaltenes as macromolecular nano-aggregates of monodispersed monomers. Hence, the asphaltene pseudo-component is divided into 30 sub-fractions, each representing a different aggregate size and the number of monomers in an aggregate or the aggregation number (r) is described by the relation:

$$r = \frac{M}{M_m} \tag{A2}$$

where M is the molar mass of the particular asphaltene aggregate or the sub-fraction, and M_m is the monomer molar mass of the asphaltenes. The gamma distribution function [49] is then used to describe the molar mass distribution of the aggregates according to the following equation as:

$$f(M) = \frac{1}{M_m \Gamma(\beta)} \left[\frac{\beta}{(\bar{r} - 1)} \right]^{\beta} \times (r-1)^{\beta-1} \exp\left[\frac{\beta(1-r)}{(\bar{r} - 1)} \right] \tag{A3}$$

where $\bar{r}$ is the average aggregation number of asphaltene fraction defined as the average molar mass of all self-associated asphaltene sub-fractions ($\overline{M}$) divided by the monomer molar mass, that is given by $\frac{\overline{M}}{M_m}$. β is a parameter that determines the shape of the distribution. The value of β is chosen as 3.5 based on an extensive data set. The molar mass of an asphaltene monomer and the largest asphaltene aggregate are assumed to be 1800 and 30,000 g/mol, respectively. Note, the asphaltene monomer molar mass of 1800 g/mol may represent an already aggregated component. Therefore, the only other input to the model is the average molar mass of all self-associated asphaltene sub-fractions ($\overline{M}$).

References

1. Mullins, O.C., et al., *Asphaltenes, Heavy Oils, and Petroleomics*. 2007: Springer.
2. Speight, J.G., *The Chemistry and Technology of Petroleum*. 1999: Taylor & Francis.
3. Eskin, D., et al., *Modeling of asphaltene deposition in a production tubing.* AIChE Journal, 2012. **58**(9): p. 2936-2948.
4. Akbarzadeh, K., et al., *Methodology for the characterization and modeling of asphaltene precipitation from heavy oils diluted with n-alkanes.* Energy and Fuels, 2004. **18**(5): p. 1434-1441.
5. Alboudwarej, H., et al., *Regular Solution Model for Asphaltene Precipitation from Bitumens and Solvents.* AIChE Journal, 2003. **49**(11): p. 2948-2956.
6. Hammami, A., et al., *Asphaltene precipitation from live oils: An experimental investigation of onset conditions and reversibility.* Energy and Fuels, 2000. **14**(1): p. 14-18.
7. Wang, J.X., et al., *A practical method for anticipating asphaltene problems.* SPE Production and Facilities, 2004. **19**(3): p. 152-160.
8. Rogel, E., C. Ovalles, and M. Moir, *Asphaltene stability in crude oils and petroleum materials by solubility profile analysis.* Energy and Fuels, 2010. **24**(8): p. 4369-4374.
9. Wiehe, I.A., *Asphaltene solubility and fluid compatibility.* Energy and Fuels, 2012. **26**(7): p. 4004-4016.
10. Wiehe, I.A. and R.J. Kennedy, *Oil compatibility model and crude oil incompatibility.* Energy and Fuels, 2000. **14**(1): p. 56-59.
11. Oliensis, G.L., *A qualitative test for determining the degree of heterogeneity of asphalts.* Am. Soc. Testing and Materials Proc., 1933. **33**(2): p. 715-728.
12. Schneider, M.H., et al., *Asphaltene molecular size by fluorescence correlation spectroscopy.* Energy and Fuels, 2007. **21**(5): p. 2875-2882.
13. Fotland, P., H. Anfindsen, and F.H. Fadnes, *Detection of asphaltene precipitation and amounts precipitated by measurement of electrical conductivity.* Proceedings of the 6th International Conference on Fluid Properties and Phase Equilibria for Chemical Process Design 1992, 1993. **82**(pt 1): p. 157-164.
14. Jamaluddin, A.K.M., et al., *Laboratory techniques to measure thermodynamic asphaltene instability.* Journal of Canadian Petroleum Technology, 2002. **41**(7): p. 44-52.
15. Escobedo, J. and G.A. Mansoori, *Viscometric determination of the onset of asphaltene flocculation: A novel method.* SPE Production & Facilities, 1995. **10**(2): p. 115-118.
16. Kharrat, A.M., et al., *Issues with comparing SARA methodologies.* Energy and Fuels, 2007. **21**(6): p. 3618-3621.
17. Sabbagh, O., et al., *Applying the PR-EoS to asphaltene precipitation from n-alkane diluted heavy oils and bitumens.* Energy and Fuels, 2006. **20**(2): p. 625-634.
18. Tharanivasan, A.K., et al., *Measurement and modeling of asphaltene precipitation from crude oil blends.* Energy and Fuels, 2009. **23**(8): p. 3971-3980.
19. Tharanivasan, A.K., H.W. Yarranton, and S.D. Taylor, *Application of a regular solution-based model to asphaltene precipitation from live oils.* Energy and Fuels, 2011. **25**(2): p. 528-538.
20. Schneider, M.H., et al., *Measurement of Asphaltenes Using Optical Spectroscopy on a Microfluidic Platform.* Analytical Chemistry, 2013. **85**(10): p. 5153-5160.
21. Hu, C., J.E. Morris, and R.L. Hartman, *Microfluidic investigation of the deposition of asphaltenes in porous media.* Lab on a Chip - Miniaturisation for Chemistry and Biology, 2014. **14**(12): p. 2014-2022.

22. Bowden, S.A., et al., *The liquid-liquid diffusive extraction of hydrocarbons from a North Sea oil using a microfluidic format.* Lab on a Chip - Miniaturisation for Chemistry and Biology, 2006. **6**(6): p. 740-743.
23. Bowden, S.A., et al., *Determination of the asphaltene and carboxylic acid content of a heavy oil using a microfluidic device.* Lab on a Chip - Miniaturisation for Chemistry and Biology, 2009. **9**(6): p. 828-832.
24. Sieben, V., A. Kharrat, and F. Mostowfi. *Novel measurement of asphaltene content in oil using microfluidic technology*. in *SPE Annual Technical Conference and Exhibition, ATCE 2013*. 2013. New Orleans, LA.
25. Hu, C. and R.L. Hartman, *High-throughput packed-bed microreactors with in-line analytics for the discovery of asphaltene deposition mechanisms.* AIChE Journal, 2014. **60**(10): p. 3534-3546.
26. Molla, S., D. Eskin, and F. Mostowfi. *Two-phase flow of gas-liquid binary mixtures through a rectangular microchannel*. in *2011 AIChE Annual Meeting, 11AIChE*. 2011. Minneapolis, MN.
27. Molla, S., D. Eskin, and F. Mostowfi, *Two-phase flow in microchannels: The case of binary mixtures.* Industrial and Engineering Chemistry Research, 2013. **52**(2): p. 941-953.
28. Mostowfi, F., S. Molla, and P. Tabeling, *Determining phase diagrams of gas-liquid systems using a microfluidic PVT.* Lab on a Chip - Miniaturisation for Chemistry and Biology, 2012. **12**(21): p. 4381-4387.
29. Fisher, R., et al., *Equilibrium gas-oil ratio measurements using a microfluidic technique.* Lab on a Chip, 2013. **13**(13): p. 2623-2633.
30. Abolhasani, M., et al., *Automated microfluidic platform for studies of carbon dioxide dissolution and solubility in physical solvents.* Lab on a Chip - Miniaturisation for Chemistry and Biology, 2012. **12**(9): p. 1611-1618.
31. Fadaei, H., B. Scarff, and D. Sinton, *Rapid microfluidics-based measurement of CO 2 diffusivity in bitumen.* Energy and Fuels, 2011. **25**(10): p. 4829-4835.
32. Kumar Gunda, N.S., et al., *Reservoir-on-a-Chip (ROC): A new paradigm in reservoir engineering.* Lab on a Chip - Miniaturisation for Chemistry and Biology, 2011. **11**(22): p. 3785-3792.
33. De Haas, T.W., et al., *Steam-on-a-chip for oil recovery: The role of alkaline additives in steam assisted gravity drainage.* Lab on a Chip - Miniaturisation for Chemistry and Biology, 2013. **13**(19): p. 3832-3839.
34. Kharrat, A.M., K. Indo, and F. Mostowfi, *Asphaltene content measurement using an optical spectroscopy technique.* Energy and Fuels, 2013. **27**(5): p. 2452-2457.
35. (ASTM), A.S.f.T.a.M., *ASTM D 6560, Standard Test Method for Determination of Asphaltenes (Heptane Insolubles) in Crude Petroleum and Petroleum Products*. 2000, American Society for Testing and Materials (ASTM): West Conshohocken, PA.
36. Wang, J. and J. Buckley, *Effect of dilution ratio on amount of asphaltenes separated from stock tank oil.* Journal of Dispersion Science and Technology, 2007. **28**(3): p. 425-430.
37. Nguyen, N.T. and Z. Wu, *Micromixers - A review.* Journal of Micromechanics and Microengineering, 2005. **15**(2): p. R1-R16.
38. Sieben, V.J., et al., *Microfluidic colourimetric chemical analysis system: Application to nitrite detection.* Analytical Methods, 2010. **2**(5): p. 484-491.
39. Maqbool, T., A.T. Balgoa, and H.S. Fogler, *Revisiting asphaltene precipitation from crude oils: A case of neglected kinetic effects.* Energy and Fuels, 2009. **23**(7): p. 3681-3686.
40. Morgado, J., et al., *Thermodynamics of interactions at infinite dilution between asphaltenes and a surfactant or crude oil resins.* Energy and Fuels, 2009. **23**(5): p. 2581-2591.
41. Ogilvie, I.R.G., et al., *Temporal optimization of microfluidic colorimetric sensors by use of multiplexed stop-flow architecture.* Analytical Chemistry, 2011. **83**(12): p. 4814-4821.

42. Karan, K., J. Ratulowski, and P. German, *Measurement of Waxy Crude Properties Using Novel Laboratory Techniques (SPE 62945)*, in *2000 SPE Annual Technical Conference and Exhibition*. 2000, Society of Petroleum Engineers: Dallas, Texas.
43. Ashoori, S., et al., *Mechanisms of asphaltene aggregation in toluene and heptane mixtures.* Journal of the Japan Petroleum Institute, 2009. **52**(5): p. 283-287.
44. Hung, J., J. Castillo, and A. Reyes, *Kinetics of asphaltene aggregation in toluene-heptane mixtures studied by confocal microscopy.* Energy and Fuels, 2005. **19**(3): p. 898-904.
45. Rajagopal, K. and S.M.C. Silva, *An experimental study of asphaltene particle sizes in n-heptane-toluene mixtures by light scattering.* Brazilian Journal of Chemical Engineering, 2004. **21**(4): p. 601-609.
46. Akbarzadeh, K., et al., *A generalized regular solution model for asphaltene precipitation from n-alkane diluted heavy oils and bitumens.* Fluid Phase Equilibria, 2005. **232**(1-2): p. 159-170.
47. Mullins, O.C., et al., *Advances in asphaltene science and the Yen-Mullins model.* Energy and Fuels, 2012. **26**(7): p. 3986-4003.
48. Wu, Q., et al., *Laser-based mass spectrometric determination of aggregation numbers for petroleum- and coal-derived asphaltenes.* Energy and Fuels, 2014. **28**(1): p. 475-482.
49. Whitson, C.H., *Characterizing hydrocarbon plus fractions.* Society of Petroleum Engineers journal, 1983. **23**(4): p. 683-694.